Photon tunnelling microscopy of polyethylene single crystals

Mohan Srinivasarao* and Richard S. Stein
Polymer Research Institute, University of Massachusetts, Amherst, MA 01003, USA

and Thomas P. Russell
IBM Research Laboratory. Almaden, San Jose, CA, USA

and John M. Guerra
Optical Engineering Division, Polaroid Corporation, Cambridge, MA, USA
(Received 28 June 1993; revised 15 September 1993)

Light incident on a total internal reflection surface will tunnel through a submicrometre gap in the presence of a dielectric surface. This tunnelling phenomenon is used in the photon tunnelling microscope to image polyethylene single crystals, providing a topographical map of the single-crystal surface. Tunnelling increases exponentially with sample height and is quantified using video photometry of the grey-scale tunnelling image.

(Keywords: photon tunnelling microscopy; single crystals; polyethylene)

INTRODUCTION

The study of morphology of polymers is an area of continuing interest in polymer science. By morphology, one means the supermolecular structure that arises from the physical organization or self-assembly of the macromolecule. On the one hand, polymers such as polyethylene, crystallized from the melt, form a spherulitic morphology, the internal structure of which has been studied in great detail[1-3]. On the other hand, polyethylene crystallized from solution gives rise to some beautiful crystal habits that have formed the basis for the understanding of the solution crystallization process in polymer materials[4-9].

It is well known that many synthetic polymers crystallized from dilute solutions form single crystals. The discovery of such 'single crystals', made almost at the same time by Keller[5], Till[6] and Fischer[7] in 1957, has had a profound impact on the understanding of crystallization of macromolecules. Their electron diffraction data showed that the polymer chains were normal to the single-crystal surface, and most remarkable, given the length of the polymer chain, was the fact that the crystals were only about 100 Å thick. This led Keller and O'Connor[8] to conclude that the molecules must fold sharply on themselves to give rise to lamellar periods of only 100 Å. Since then several studies have been carried out on solution-grown crystals, always confirming and elaborating on the rather remarkable phenomenon of chain folding leading to the single-crystal habit.

The principal tool that has been used to study the morphology of single crystals is electron microscopy and diffraction either from electrons or X-rays. Despite its obvious importance, electron microscopy is not without its shortcomings. These include the relatively high cost, the need for high vacuum, loss of the ability to manipulate samples, and possible damage to samples upon irradiation with the electron beam. These limitations are overridden in many cases by the resolution achievable and by the fact that one can perform selected-area diffraction to determine the unit-cell structure and orientation of crystalline polymers. Nevertheless, in an effort to circumvent many of the limitations of electron microscopy, Wunderlich and coworkers[10] and others[11,12] have used several forms of interference microscopy to visualize the single crystals formed from solution. All forms of interference microscopy use the phase difference between a ray of light split into two or more rays, which on passing through a polymer crystal are made to recombine at a later stage, in the microscope, into a single ray. This phase difference is then converted into an intensity difference, thus making the polymer crystal visible and in some cases even leading to quantitative measurements of the thickness of the lamellae[10].

Photon tunnelling microscopy (p.t.m.), described fully elsewhere[13], is proving to be a valuable tool for the characterization of topographical features of many dielectric surfaces including polymers. P.t.m., a form of optical microscopy descended from surface contact microscopy[14] and frustrated total internal reflection microscopy (f.t.i.r.m.)[15], makes use of evanescent waves to image topographical features with a height resolution of less than a nanometre and a lateral resolution of 0.16 μm. The image is displayed in high-resolution 3D with continuously varying perspective (see *Figures 4* and *5*).

It is well known that a light beam propagating in medium 1 with refractive index n_1 incident on a boundary

* To whom correspondence should be addressed

0032-3861/94/06/1137-05

with medium 2 having a lower refractive index n_2 undergoes total internal reflection at a critical angle given by $\sin^{-1}(n_2/n_1)$. As no energy is transferred into the rarer medium, the field in medium 2 is termed an evanescent wave. The amplitude of this wave decays exponentially with distance z normal to the reflecting boundary and the field strength E_{ev} of this decay is given by:

$$E_{ev} = E_0 \exp(-z/d_p) \quad (1)$$

where E_0 is the amplitude of the electric field associated with the light beam in medium 1 at the boundary. The penetration depth d_p in medium 2 at which the amplitude E_0 decreases by a factor 1/e is given by:

$$d_p = \frac{\lambda_1}{2\pi(\sin^2\theta - n_{21}^2)^{1/2}} \quad (2)$$

where λ_1 is the wavelength in the denser medium 1, θ is the incident angle and $n_{21} = n_2/n_1$. In the presence of a third medium with refractive index $n_3 > n_2$, the total reflection is frustrated. The third medium leads to the conversion of the evanescent wave to a propagating wave by an amount that is exponentially proportional to the distance z from the totally reflecting surface. If the surface of this medium is topographically rough, this causes a change in the total reflection, leading to a frustration of total reflection, which may differ from place to place laterally owing to the local variation of the surface topography. This results in the modulation of the intensity of the reflected light corresponding spatially to the modulation of z by the surface topography of the third (dielectric) medium. This produces a grey-scale image where height information is mapped onto an intensity distribution. Photometry of this grey-scale image (or intensity distribution) yields quantitative height measurements directly and without ambiguity. The brighter the image, the further the feature is from the total internal reflection (t.i.r.) surface. It is important to note that the remarkable sensitivity to height variations originates from the exponential dependence of the frustration of total reflection on depth. This leads to a sub-nanometre detector-limited resolution in the z direction. Hence, the surface topography can be obtained from photometry of the tunnelling image, if the exact dependence of the energy transfer on z is known. This dependence can be calculated *a priori* for non-absorbing dielectrics, but is difficult to do for other classes of materials. Conversely, this dependence can be empirically calibrated, as was done elsewhere[13]. The vertical resolution of height variation is limited only by detector discrimination of the corresponding intensity modulation of the tunnelling image.

EXPERIMENTAL

The optical microscope (Nikon or equivalent) is equipped with vertically incident Kohler illumination, a phototube and a reflected-light oil immersion objective of numerical aperture (*NA*) 1.25 and 100× magnification, and is schematically shown in *Figure 1*. A microscope coverglass serves to hold the oil for the immersion objective and also serves as the object plane for t.i.r. In some cases it has been useful to use a thin proprietary (Polaroid) flexible optical membrane as the transducer (or the object plane for t.i.r.) that is stiff over the field of view of the microscope but flexible enough on a larger scale to accommodate curved surfaces and even dirt on the sample. The microscope stage is used for the vertical motion of the sample. A photometric vidicon camera (Dage MTI, Series, 81) mounted on the phototube converts the grey-scale tunnelling image into a video signal that is restored into a real-time 3D image of the sample topography by a three-axis oscilloscope. At the present time, the vidicon detector produces a vertical resolution better than 1 nm (a fraction of a nanometre)[13]. This was determined using a calibration mapping function generated from a smooth glass sphere of 1.6 m radius[13]. To demonstrate the capability of the microscope, images of a moulded optical storage structure obtained using a p.t.m., microinterferometer (Wyko Corporation), scanning electron microscope (SEM) and atomic force microscope (a.f.m.) are shown in *Figure 2*.

Polyethylene (Marlex-50) was crystallized from a dilute (0.5%) *p*-xylene solution at 80°C to obtain large single crystals. A small amount of the suspension of *p*-xylene containing the single crystals was deposited on a microscope slide and the solvent was removed by evaporation under atmospheric conditions. Images of several crystals on the slide were obtained with the photon tunnelling microscope.

RESULTS AND DISCUSSION

Figure 3 shows the grey-scale image of a polyethylene single crystal as viewed directly under the p.t.m., where the individual single crystals are visible as intensity differences in the grey-scale image. The high resolution and contrast of this image is rather remarkable, as viewed through the microscope. In order to quantify the

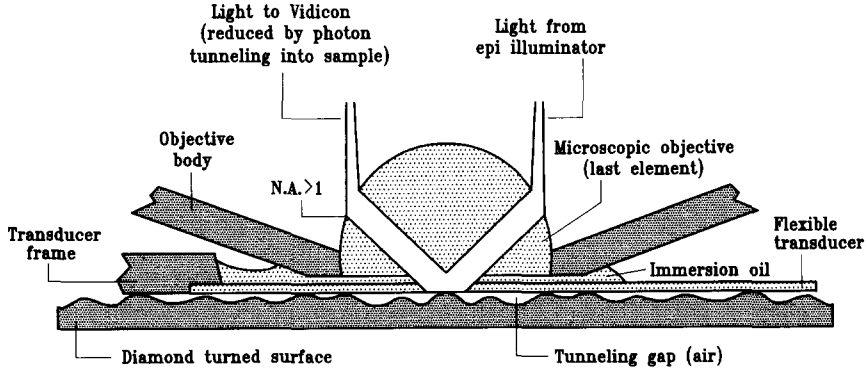

Figure 1 Schematic of the principle of operation of the photon tunnelling microscope

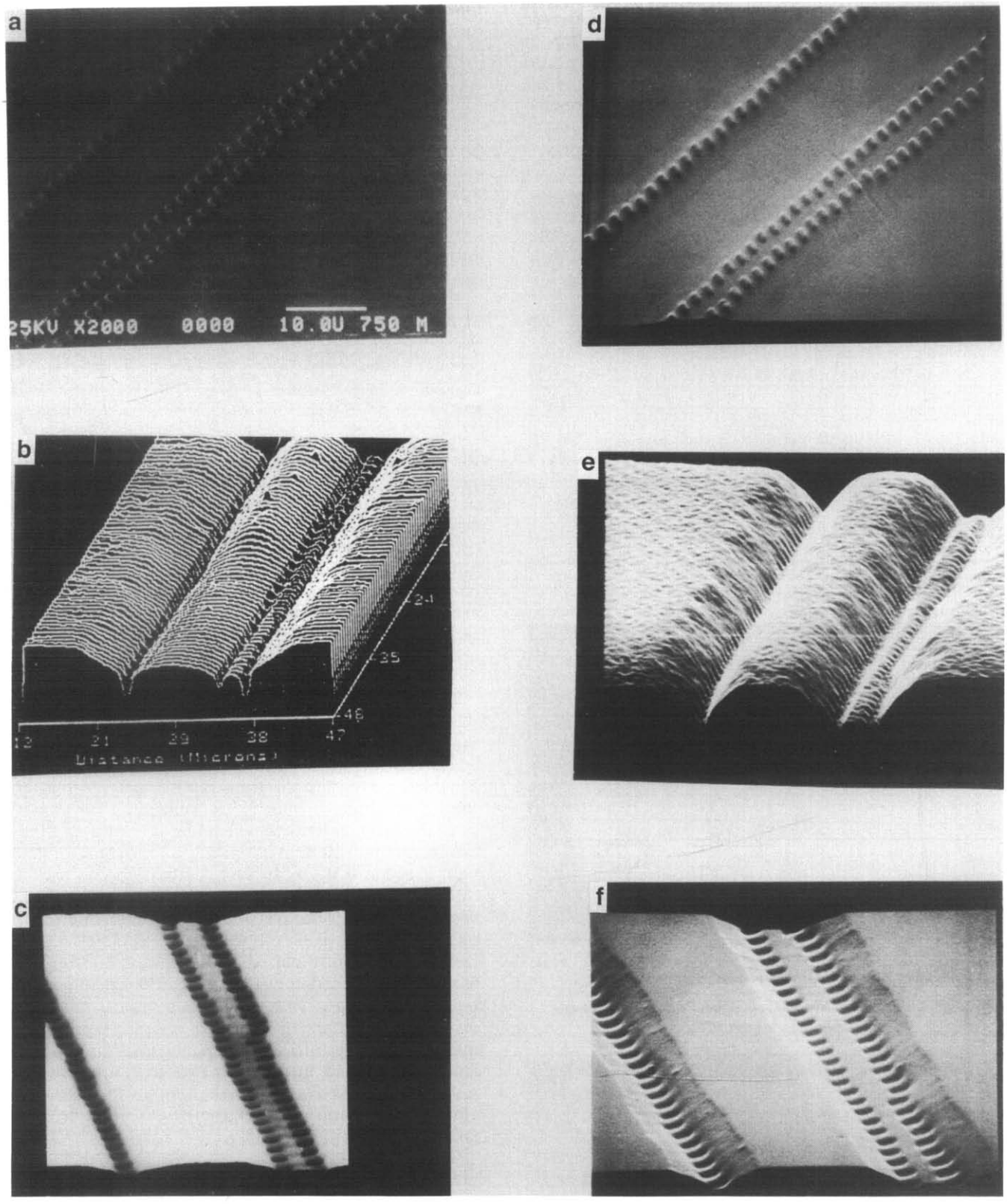

Figure 2 Comparison images obtained of an optical storage disc: (a) SEM, (b) Wyko and (c) a.f.m. images; (d), (e), (f) corresponding p.t.m. images

tunnelling image, a charge-coupled device (c.c.d.) or a vidicon detector views the tunnelling image at the microscope's phototube in the normal manner. This output is readily analysed and displayed in any number of ways. *Figure 4* shows the analogue 3D display of the grey-scale image shown in *Figure 3*. The single terraces of the polyethylene crystals are very clearly seen in this figure. Each video raster line of a high-resolution XY oscilloscope is displayed as amplitude traces, thus electronically mapping the intensity distribution of the grey-scale image into height for a real-time 3D image. A single trace can be isolated anywhere in the image for electronic cross-sectioning and height measurement. The terraces of the single crystal are easily seen and have step

heights of ~7 nm. It should be emphasized that the image in *Figure 4* is obtained without any shadowing or extraneous sample preparation methods normally used in a SEM, for example. The contrast is provided by the tunnelling probability of the light beam being exponentially dependent on the z direction.

A further advantage of using the analogue display is the ease of manipulating the image. For example, the perspective of the image can be changed, which can aid in the understanding of the topography. An image of the single crystal obtained by expanding the scale of the oscilloscope is shown in *Figure 5*. It should be pointed out that the apparent height in the 3D image, in comparison to the lateral dimensions, is markedly exaggerated, as is often the case with most profilometry techniques. The long side of the photograph is 25 μm across, while the step heights are only on the order of 7.0–8.0 nm.

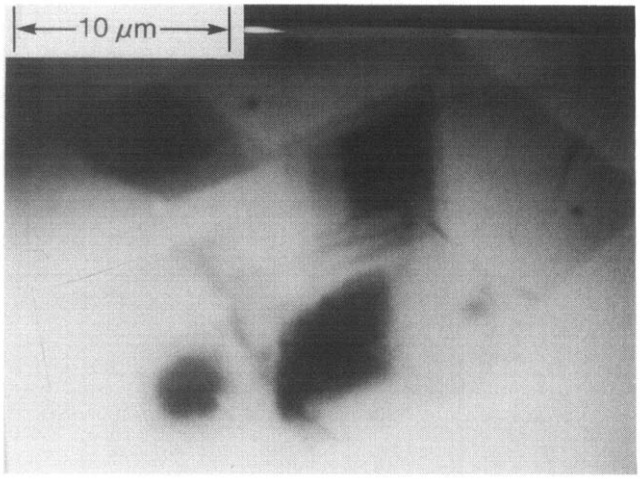

Figure 3 Tunnelling image of polyethylene single crystals as seen through the p.t.m.

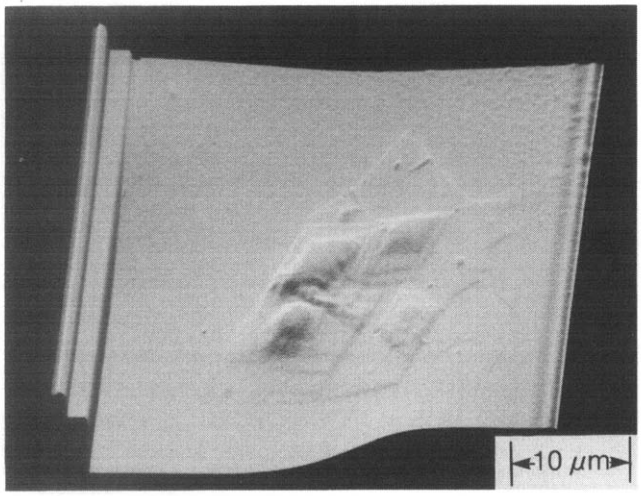

Figure 4 Topography (3D image) of polyethylene single crystals

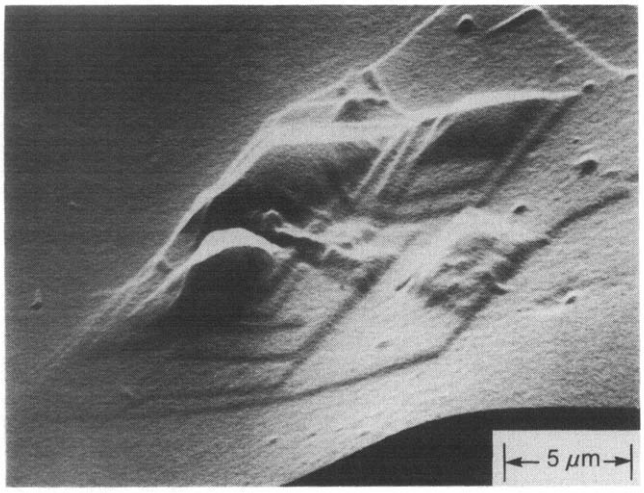

Figure 5 An expanded view showing only the single crystals

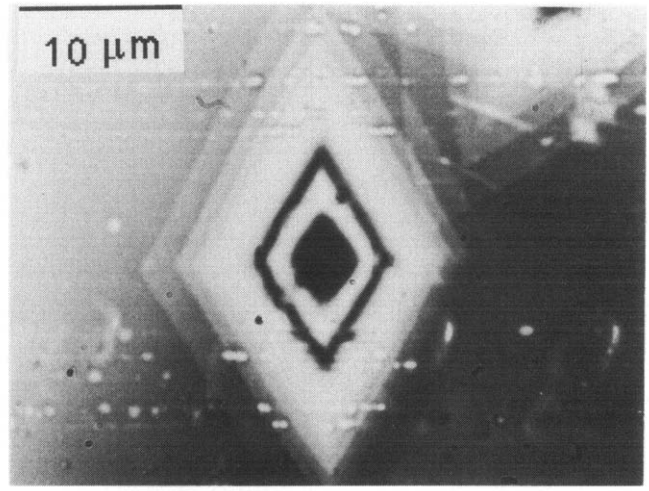

Figure 6 A contact interference image of the polyethylene single crystals obtained by suppression of t.i.r. illumination of the p.t.m.

Frequently the height of the single crystals exceeded the tunnelling range. This was due primarily to the fact that many of the crystals had a centre of the growth spiral that was much thicker than the rest of the crystal. This lifted the flexible transducer much beyond the tunnelling range. A limit to the tunnelling range exists since the probability with which t.i.r. is frustrated decays exponentially. This limit is typically 0.75λ, which for green light is about 0.38 μm. In such a situation one uses the other attributes of the microscope to image the thicker crystal, for example conversion of p.t.m. to an interference microscope. This is accomplished by suppression of the t.i.r. illumination, required for interferometry, and refocusing the microscope to image the crystal in the interference mode. Now, the flexible optical membrane serves as a contact interference reference surface. An interference image of a single crystal consisting of several lamellae obtained using the p.t.m. in the interference mode is shown in *Figure 6*. Use of monochromatic light allows for quantification of the height of each of the lamellae.

The fact that the p.t.m. is easily adaptable to do interference microscopy implies that one has not only a method to observe large single crystals, and possibly dendrites, but also a method to determine the lamellae thickness and indices of refraction. Wunderlich and coworkers[10] demonstrated these aforementioned capabilities previously. Though not done here, it is also possible from the measurement of indices of refraction to determine the chain orientation within the crystal.

CONCLUSIONS

It has been shown that photon tunnelling microscopy can yield quantitative information on the topography of

polymer surfaces, in particular of single crystals of polyethylene. In cases where the peak-to-valley variation of the surface topography exceeded the limits of the technique, simple interference microscopy could be used to complement the tunnelling method.

ACKNOWLEDGEMENT

We acknowledge support from NSF Grant DMR-9101323.

REFERENCES

1 Stein, R. S. in 'Growth and Perfection of Crystals' (Eds. Doremus, Roberts and Turnbull), Wiley, New York, 1958
2 Stein, R. S. and Rhodes, M. B. *J. Appl. Phys.* 1960, **31**, 1873
3 Keith, H. D. and Padden, F. J. *J. Appl. Phys.* 1963, **34**, 2409
4 Bassett, D. C. 'Principles of Polymer Morphology', Cambridge University Press, Cambridge, 1981, Ch. 3
5 Keller, A. *Phil. Mag.* 1957, **2**, 1171
6 Till, P. H., Jr *J. Polym. Sci.* 1957, **24**, 301
7 Fischer, E. W. *Z. Naturforsch.* 1957, **120**, 753
8 Keller, A. and O'Connor, A. *Discuss. Faraday Soc.* 1958, **25**, 114
9 Geil, P. H. 'Polymer Single Crystals', Wiley-Interscience, New York, 1963
10 Sullivan, P. and Wunderlich, B. *SPE Trans.* 1964, **4**, 2
11 Sullivan, P. and Wunderlich, B. *Polym. Lett.* 1964, **2**, 537
12 Reneker, D. H. and Geil, P. H. *J. Appl. Phys.* 1960, **31**, 1916
13 Guerra, J. M. *Appl. Opt.* 1990, **29**, 3741
14 Ambrose, E. J. *Nature* 1956, **178**, 1194
15 McCutchen, C. W. *Rev. Sci. Instrum.* 1964, **35**, 1340